

(-)-Menthol- β -cyclodextrin inclusion complex production and characterization

Guangyong Zhu¹, Zuobing Xiao^{1,2,*}, Rujun Zhou¹, Junhua Liu¹, Guangxu Zhu³, Xiongjian Zheng⁴

¹Shanghai Institute of Technology, No. 100 Haiquan Road, Shanghai, 201418, PR China

²Shanghai Jiao Tong University, No. 800 Dongchuan, Road, Shanghai, 200240, PR China

³3035 Sable Ridge Dr. Ottawa, ON K1T 3R9, Canada

⁴ShangHai LanHic Biotech Co., Ltd., No. 1165 Jindu Road, Shanghai, 201108, PR China

*Corresponding author: e-mail: zbingxiao@sina.com

(-)-Menthol has been widely used in clinical medicine, flavor, and fragrance. However, high volatility, short retention time, low solubility in water, and whisker growth of menthol are crucial problems for its application. In this paper, (-)-menthol- β -cyclodextrin inclusion complex was fabricated to solve these problems. The product was characterized by X-ray diffraction, Fourier transform infrared spectroscopy and thermogravimetric analysis. The results showed that menthol was successfully encapsulated in the cavity of β -cyclodextrin. Menthol itself vaporized almost completely at around 120 °C, while the maximum menthol release rate occurred at 267.5 °C after the formation of the inclusion complex. The stability and retention time were improved. The menthol release reaction order, apparent activation energy and the pre-exponential factor were obtained and their values were 0, 142.9 kJ/mol and 1.6×10^{13} respectively. The structure of menthol- β -cyclodextrin inclusion complex was investigated by molecular simulation and the minimum energy, -116.7 kJ/mol, was obtained at -0.8×10^{-10} m.

Keywords: Menthol- β -cyclodextrin inclusion complex; Preparation; Characterization; Kinetics; Molecular mechanics

INTRODUCTION

Menthol, also called 5-menthyl-2-(1-methylethyl)-cyclohexanol, is a monocyclic terpene alcohol as shown in Fig. 1.

Because of three asymmetric carbon atoms in its cyclohexane ring, menthol has four pairs of optical isomers, i.e. (-) and (+) menthol, isomenthol, neoisomenthol and neomenthol. Among these isomers, (-)-menthol, the main component of cornmint and peppermint oils, is the isomer that occurs most widely in nature. (-)-Menthol, with a melting range of 41–44 °C, exerts a cooling and refreshing effect and has a characteristic peppermint odor. The other isomers do not possess the characteristic peppermint odor and the cooling effect. Therefore, (-)-menthol is the one commonly identified as menthol¹.

The taste threshold of menthol is low. Taste characteristics of menthol at 25 ppm are camphoreous, cooling, minty with a clean eucalyptus note². Menthol plays an important role in consumer choice and sensory evaluation, although it usually accounts for a tiny proportion of a final product composition³. Due to its characteristic odor, menthol has been widely used in a lot of products such as foods, beverages, confectionaries, mouthwashes, toothpastes, pharmaceuticals, and cigarettes as a flavoring ingredient^{3,4}.

Since the 1920s, menthol, as an additive in tobacco, has been marketed in the US⁵. Because of anesthetic and

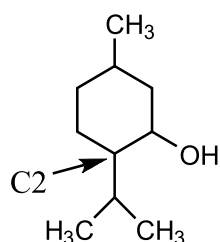


Figure 1. The structure of 5-menthyl-2-(1-methylethyl)-cyclohexanol

cooling properties of menthol, when added to tobacco, menthol has been postulated to add flavor to smoke, reduce harshness and soothe the taste, and mask nicotine's irritation⁶. It is the most significant flavoring additive in many tobacco products. Menthol can modulate the function of several ionotropic neurotransmitter receptors^{5,7}.

Because of its relative safety and high efficiency, menthol has been widely used in clinical medicine as a penetration enhancer. High concentrations of menthol can fluidize the stratum corneum lipids and enhance permeability. Through direct interactions of menthol with lipids, the penetration enhancement can take place⁸. Without causing toxic reactions, menthol can be used to improve the ocular penetration of a drug in a transscleral and transcorneal drug delivery system⁹. A menthol/borneol (75:25) eutectic mixture can effectively enhance the absorption of daidzein which can be used to reduce breast cancer occurrence and protect against colon cancer¹⁰. 0.1% menthol ozone eye drops can reduce corneal dissolving area and corneal opacity, inhibit corneal neovascularization area. Menthol, as a permeability enhancer, can increase the bioavailability of ozone ophthalmic solution and improve its therapeutic effect¹¹.

l-menthol can override thermal homeostasis to enable the achievement of a higher workload. Oral l-menthol can reduce thermal sensation, extend time to exhaustion, and increase work-rate, in the heat at a fixed rating of perceived exertion¹². Body sprays comprising 0.05–0.8% menthol solution have been shown to induce improvements in thermal sensation and comfort during fixed intensity and self-paced exercise in the heat. The performance can be enhanced by using a relatively low concentration of menthol solution¹³. Menthol cream can be used for relieving muscular fatigue and thermal discomfort after intensive exercise. It can be effectively applied to sports therapy during recovery¹⁴. During steady state exercise, previously applied menthol on the skin can induce vasoconstriction, delay initiation of sweating and reduce the sweating gain¹⁵.

Menthol is an effective antifungal ingredient. Especially, it has an obvious inhibitory effect on *Sclerotinia sclerotium*, *Rhizopus stolonifer* and *Mucor*. Menthol has obvious anti-tumor activity. It has inhibitory effect on the growth of human bladder cancer cell and cloned colon adenocarcinoma cell, the migration of prostate cancer cell and the proliferation of gastric cancer SGC-7901¹⁶. Due to the antifungal, antibacterial and probable anti-inflammatory effects of menthol, topical application of menthol is an effective method in treatment of candidal napkin dermatitis¹⁷. Menthol can also be used in the treatment of chronic cholecystitis¹⁸. During colonoscopic examination which is an effective approach for the diagnosis, detection, and treatment of colorectal neoplastic lesions, colonic spasm impedes accurate diagnosis and therapy. 0.8% L-menthol solution is effective in preventing colonic spasm¹⁹. Lotions and creams containing 1–5% menthol have been used for decades to quickly relieve pruritus. Menthol can increase the number of hair follicles and dermal thickness in the depilated area, promote hair elongation, and prolong the anagen hair cycle in mice²⁰. Menthol is an effective anesthetic that has been used for many fish species. The concentrations of menthol between 50 and 125 mg L⁻¹ can be used for the African cichlid *Aulonocara nyassae*²¹.

(-)-Menthol is fused mass or crystalline powder, usually needle-like at room temperature. It is slightly soluble in water and very soluble in alcohol and volatile oils. Because menthol is easy to sublime and volatilize, it can cause strong irritation during the production process and can influence shelf life of menthol. Menthol whisker can cause the lowering of the medication quantity in tablet, and the reduction of the mixing degree and fluidity in powder in the medical preparation⁴. If menthol is administered orally for treatment, it should preferably be prepared with a coating to avoid irritating the mucous membranes. High volatility, short retention time, very low solubility in water, and whisker growth of menthol are crucial problems for its application^{4, 22, 23}. Molecular encapsulation in cyclodextrin seems to be useful to solve these problems. Because of its natural origin, low toxicity, good water solubility and biocompatibility, β -cyclodextrin is an attractive coating material to accommodate a variety of organic molecules²⁴. β -cyclodextrin, as a protecting shell, can encapsulate molecules in its hydrophobic cavity to improve their stability and shelf life, provide long-lasting effect, enhance the solubility and bioavailability of the guest molecules^{25–27}.

In this study, (-)-menthol- β -cyclodextrin inclusion complex was fabricated by molecular encapsulation to solve these problems mentioned above. The inclusion complex was determined by X-ray diffraction and Fourier transform infrared spectroscopy to see if menthol was encapsulated in β -cyclodextrin and amorphous or crystalline. To understand the structure of the inclusion complex and the connection between menthol and β -cyclodextrin, molecular mechanics calculations were adopted to investigate the geometries and to obtain the binding energies. Thermogravimetric analysis was used to investigate kinetic parameters and long-lasting propriety of menthol after encapsulation.

MATERIALS AND METHODS

Materials

(-)-Menthol (C₁₀H₂₀O, molecular weight 156, pharmaceutical grade, colorless crystal) was provided by Guangzhou Levon Flavor & Fragrance Technology Co., Ltd. β -cyclodextrin (C₄₂H₇₀O₃₅, molecular weight 1134, white crystalline powder, pharmaceutical grade) came from Shandong Binzhou Zhiyuan Bio-Technology Co., Ltd. Anhydrous ethyl alcohol (analytical grade) was purchased from Shanghai Sinopharm Chemical Reagent Co., Ltd. Distilled water adopted throughout the experiments was manufactured in our laboratory. Without further purification, all the raw materials were directly used in the experiment.

The encapsulation process of (-)-menthol in β -cyclodextrin to form inclusion complex

With some modifications, the precipitation method of preparation of inclusion complexes with β -cyclodextrin as a coating material was used to encapsulate menthol as mentioned in references^{27, 28}. Firstly, β -cyclodextrin (10 g) was dispersed in distilled water (80 g) at 45 °C to form a suspension, to which 3 g of menthol was then added slowly. After menthol was completely added, the suspension was stirred for 3 hours at the temperature of 45 °C. Then, the suspension was stored in a refrigerator for 24 hours at the temperature of 5 °C. The precipitate was obtained by vacuum filtration and was washed with anhydrous ethyl alcohol. A freeze drier (FD-1C-50) was adopted to dry the precipitate. The dry time, temperature and pressure were 24 hours, lower than -50 °C, about 24 Pa respectively. A desiccator was used to store the dried menthol- β -cyclodextrin inclusion complex for further analysis.

Characterization of menthol- β -cyclodextrin inclusion complex

The menthol- β -cyclodextrin inclusion complex was characterized by morphology, Fourier transform infrared spectroscopy (FTIR), x-ray diffraction (XRD) and thermogravimetric analysis (TGA) respectively. The morphology of the product was observed with an XSP-BM19A optical microscopy (Shanghai optical instrument factory, China) as described in reference²⁸. A Vertex 70 Fourier transform infrared spectrometer (Bruker, Germany) was adopted to obtain the FTIR spectra of the samples. A D/Max 2000X X-ray diffractometer (Rigaku Corporation, Japan) was used to investigate XRD patterns of the samples and the operating conditions were used as described in reference²⁷. Mass loss and rate of mass loss were carried out with a TGA-Q5000IR thermogravimetric analyzer (TA Instruments, USA). The operation conditions were also adopted as mentioned in reference²⁷. The heating rate for the pyrolysis of samples was 10 °C/min. N₂, as an inert gas, was used during the pyrolysis process.

Molecular simulation of the interaction of menthol and β -cyclodextrin

The method of molecular simulation of the interaction of menthol and β -cyclodextrin was adopted as literatures^{22, 28, 29} with some modifications. The structures and energies calculations for investigation of the interaction of menthol and β -cyclodextrin were studied using Chem3D Ultra (CambridgeSoft Corporation, MA, USA). The Chem3D provides computations using the molecular mechanics force field. Based on molecular mechanics (MM), molecular structures were optimized and molecular energies were calculated. Menthol moved along Z axis to the cavity of β -cyclodextrin as shown in Fig. 2. The Z coordinate of carbon atom (C2) of menthol was used to express the position between menthol and β -cyclodextrin. By successively changing the Z coordinate of menthol, the inclusion process was simulated and the energy was minimized by MM2.

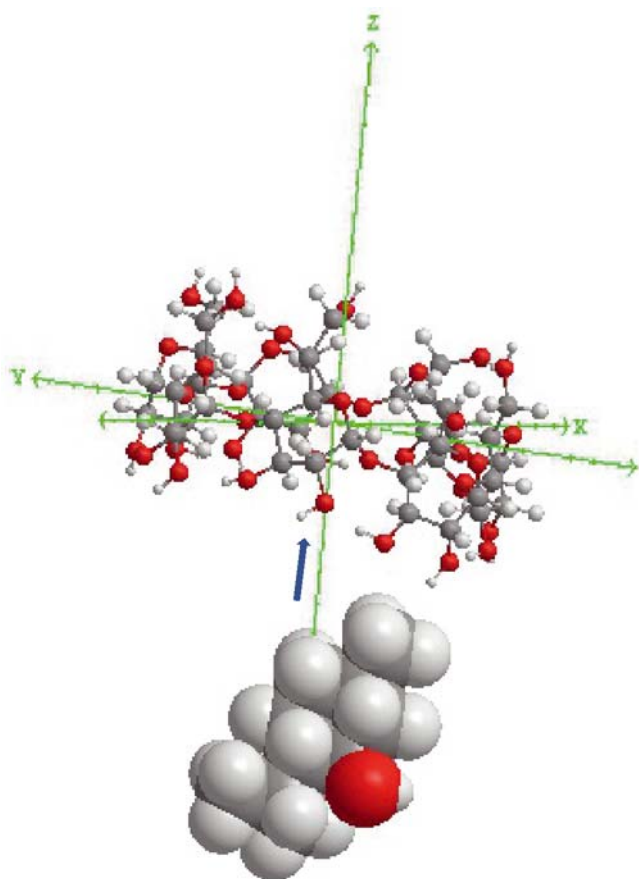


Figure 2. Menthol moving direction during the formation of the menthol- β -cyclodextrin inclusion complex

RESULTS AND DISCUSSION

The appearance of menthol- β -cyclodextrin inclusion complex

Menthol- β -cyclodextrin inclusion complex was observed with an XSP-BM19A optical microscopy. The appearance of menthol- β -cyclodextrin inclusion complex is different in both shape and size as shown in Fig. 3. Due to the aggregation of β -cyclodextrin in aqueous suspension, some large aggregates of about 20 μm can be found in Fig. 3. Among these aggregates, some of them resemble parallelograms and rhombuses in shape, which might

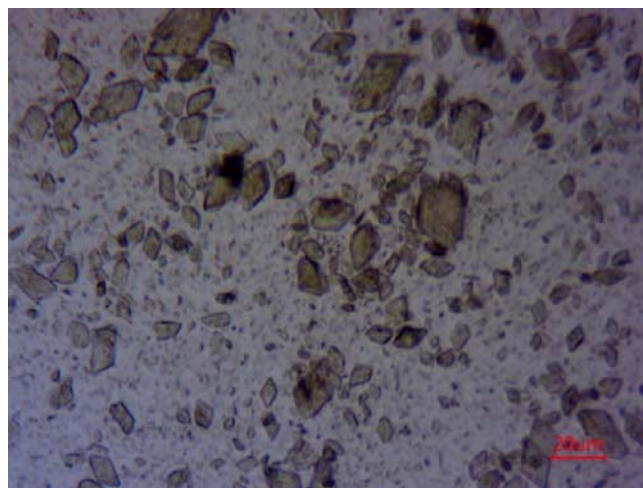


Figure 3. The image of menthol- β -cyclodextrin inclusion complex

result that the cyclodextrin complexes prefer to line up in staggered parallel arrangements as shown in Fig. 4. This is because the energy surface for the staggered parallel arrangement is attractive. It is energetically favorable for the β -cyclodextrin complexes to line up in staggered parallel arrangement³⁰. Therefore, the β -cyclodextrin inclusion complexes may be stacked in layers like bricks as shown in Fig. 4. The menthol- β -cyclodextrin inclusion complex aggregates with parallelogram or rhombuses shapes may be formed in this way³¹.

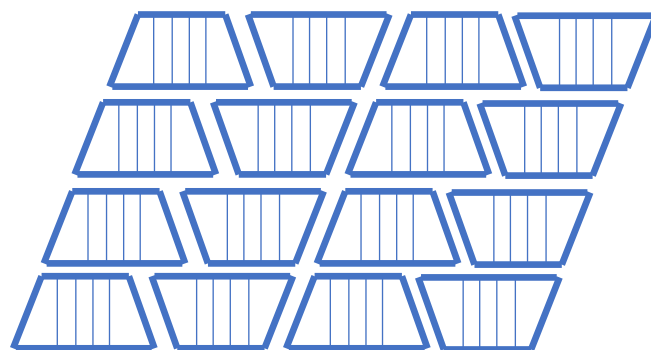


Figure 4. Schematic description of cyclodextrin complexes in staggered parallel arrangement

FTIR results of (-)-menthol- β -cyclodextrin inclusion complex, β -cyclodextrin and (-)-menthol

A Vertex 70 Fourier transform infrared spectrometer was used to obtain the FTIR spectra of (-)-menthol- β -cyclodextrin inclusion complex, β -cyclodextrin and (-)-menthol and the results are shown in Fig. 5.

As shown in Fig. 5, the peaks at 3252 cm^{-1} (due to the stretching O-H vibration), 2922 and 2870 cm^{-1} (due to the stretching C-H vibration), and 1454 cm^{-1} (due to the deformation C-H vibration)²² in the curve of menthol disappear in the curve of menthol- β -cyclodextrin inclusion complex. The peak at 3362 cm^{-1} (due to the stretching O-H vibration of hydroxyl group) in the curve of β -cyclodextrin shifts to 3300 cm^{-1} in the curve of menthol- β -cyclodextrin inclusion complex. After the formation of the inclusion complex, the peak moves towards the low-band and blue shift can be observed. The changes in peak position, peak shape, and intensity of FTIR reflect the nature of the interaction and can

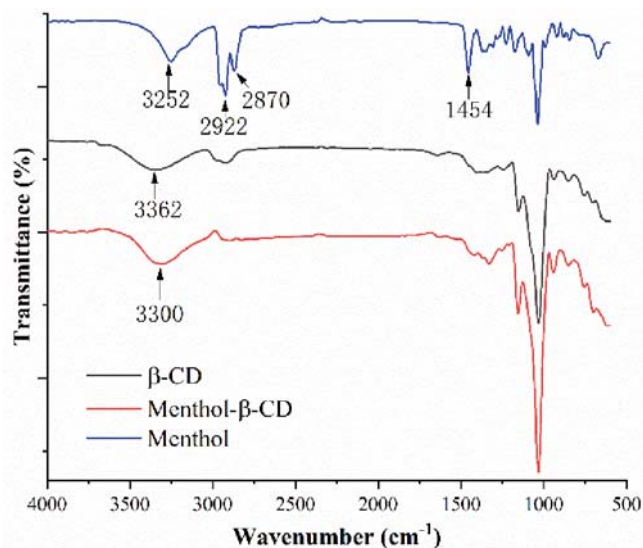


Figure 5. FTIR results of (-)-menthol- β -cyclodextrin inclusion complex, β -cyclodextrin and (-)-menthol

be used to deduce whether the guest molecule enters the cavity of β -cyclodextrin or not³². These changes in peaks provide evidence that menthol was encapsulated in the cavity of β -cyclodextrin.

XRD results of (-)-menthol- β -cyclodextrin inclusion complex, β -cyclodextrin and (-)-menthol

XRD is a useful method of determination of the formation of the solid guest-host inclusion complexes. Some characteristic peaks of a crystal guest will disappear or decrease in intensity after the formation of guest-host inclusion complex. Furthermore, peaks of β -cyclodextrin will also change. These phenomena can be used to deduce whether the guest molecule enters the cavity of β -cyclodextrin or not³². A D/Max 2000X X-ray diffractometer was used to investigate XRD patterns of the (-)-menthol- β -cyclodextrin inclusion complex, β -cyclodextrin and (-)-menthol and the results are shown in Fig. 6.

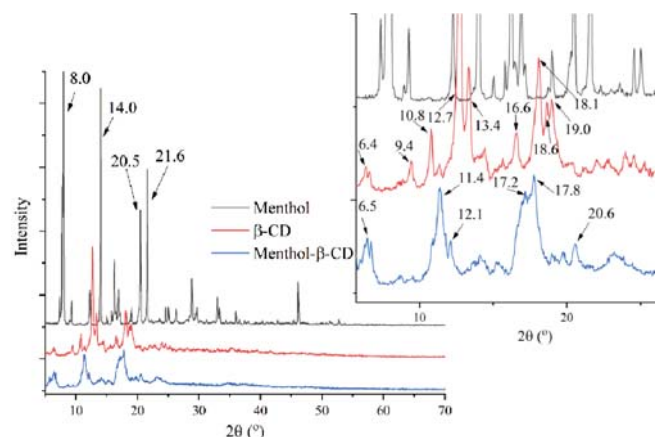


Figure 6. XRD results of (-)-menthol- β -cyclodextrin inclusion complex, β -cyclodextrin and (-)-menthol

As shown in Fig. 6, four relatively strong sharp peaks appear at 8.0, 14.0, 20.5, and 21.6° in the XRD curve of menthol. However, there are no peaks appearing at 8.0, 14.0, and 20.5° in the XRD curve of menthol- β -cyclodextrin inclusion complex. Probably due to menthol having a peak at 20.5°, a small peak appears at 20.6°

in the XRD curve of menthol- β -cyclodextrin inclusion complex, while this peak does not occur in the XRD curve of β -cyclodextrin. Furthermore, the peaks at 9.4, 10.8, 12.7, 13.4, 16.6, 18.1, 18.6, and 19.0° in the XRD curve of β -cyclodextrin disappear in the XRD curve of menthol- β -cyclodextrin. However, some new peaks occur at 11.4, 12.1, 17.2, and 17.8° in the XRD curve of menthol- β -cyclodextrin inclusion complex. From these changes, it can be inferred that menthol molecules are encapsulated in the cavities of β -cyclodextrin molecules.

Pyrolysis characteristics of (-)-menthol, β -cyclodextrin and (-)-menthol- β -cyclodextrin inclusion complex

Pyrolysis characteristics can be used to measure the combination of host and guest molecules. Mass loss and rate of mass loss of (-)-menthol, β -cyclodextrin and (-)-menthol- β -cyclodextrin inclusion complex were carried out with a TGA-Q5000IR thermogravimetric analyzer and the results are shown in Fig. 7.

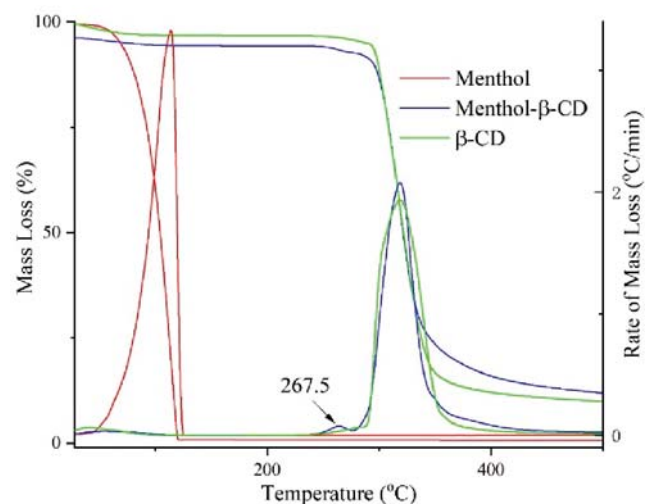


Figure 7. Mass loss and rate of mass loss of (-)-menthol, β -cyclodextrin and (-)-menthol- β -cyclodextrin inclusion complex

As shown in Fig. 7, there are three strong peaks in the curves of rate of mass loss. One peak appears at 114.0 °C due to the volatilization of (-)-menthol and the other two peaks occur at 318.7 °C due to the decomposition of β -cyclodextrin. From Fig. 7, we can see that the temperature of initial decomposition of β -cyclodextrin is about 297.8 °C. The two strong sharp peaks observed at 318.7 °C in the curves of the rate of mass loss of β -cyclodextrin and (-)-menthol- β -cyclodextrin inclusion complex mean that the decomposition rate of β -cyclodextrin attains the maximum value. As shown in Fig. 7, (-)-menthol vaporized quickly with the increase of temperature. The strong sharp peak observed at 114.0 °C in the curve of the rate of mass loss of (-)-menthol means that the rate of mass loss of menthol attains the maximum value. Menthol vaporized almost completely at around 120 °C. Compared with β -cyclodextrin, a small peak appears at 267.5 °C in the curve of the rate of mass loss of (-)-menthol- β -cyclodextrin inclusion complex. However, there is no peak in the curve of the rate of β -cyclodextrin at this temperature. It indicates that (-)-menthol is the cause of this peak, and further confirms that (-)-menthol is encapsulated in the cavity of β -cyclodextrin. During the

pyrolysis of (-)-menthol- β -cyclodextrin inclusion complex, the release of (-)-menthol still occurs before the temperature of initial decomposition of β -cyclodextrin and the maximum (-)-menthol release rate appears at 267.5 °C. During the heating process of (-)-menthol itself, it vanished when the temperature exceeded 120 °C. From these phenomena, it can be inferred that the formation of inclusion complex can improve the thermo stability of (-)-menthol and provide a long-lasting effect.

Thermogravimetric kinetics can be used for exploration of the combination of (-)-menthol and β -cyclodextrin. (-)-Menthol release activation energy can be thought as the energy barrier separating (-)-menthol from (-)-menthol- β -cyclodextrin inclusion complex. (-)-Menthol release reaction model in reference²² can be used to express (-)-menthol release during heating of (-)-menthol- β -cyclodextrin inclusion complex. The kinetic parameters of (-)-menthol release from its inclusion complex can be evaluated using thermogravimetric data. Based on Coats and Redfern method^{22, 27}, Eqs (1) and (2) can be adopted to determine the kinetic parameters, such as apparent active energy, reaction order and pre-exponential factor.

$$\ln \left[\frac{1-(1-\alpha)^{1-n}}{T^2(1-n)} \right] = \ln \left(\frac{AR}{\beta E} \right) - \frac{E}{RT} \quad (\text{for } n \neq 1) \quad (1)$$

$$\ln \left[\frac{-\ln(1-\alpha)}{T^2} \right] = \ln \left(\frac{AR}{\beta E} \right) - \frac{E}{RT} \quad (\text{for } n=1) \quad (2)$$

where α is the fraction of (-)-menthol- β -cyclodextrin inclusion complex decomposed at time t , n is the reaction order, T is the absolute temperature, R is the gas constant, A is the pre-exponential factor, β is the heating rate, and E is the apparent activation energy.

For a correct value of n , a straight line of slope $-E/R$ should be obtained from a plot of either $\ln[-\ln(1-\alpha)/T^2]$ against $1/T$ or, where $n \neq 1$, $\ln[(1-(1-\alpha)^{1-n})/T^2/(1-n)]$ against $1/T$. According to Eqs. (1) and (2), the squared values of linear correlation coefficient (R^2) for various reaction orders can be obtained by fitting the thermogravimetric data and the results are shown in Table 1.

As shown in Table 1, among the squared values of linear correlation coefficient (R^2) 0.9952 is the closest value to 1. The closer is the R^2 to 1, the better the linear relationship should be. Therefore, 0 is adopted as the (-)-menthol release reaction order. The (-)-menthol release shows the kinetic characteristic of zero-order reaction.

For $n=0$, the plot of $\ln[(1-(1-\alpha))/T^2]$ against $1/T$ is shown in Fig. 8. A good linear relationship can be observed in Fig. 8. The apparent activation energy and the pre-exponential factor can be calculated from the slope and the intercept of the line respectively. based on Eq. (1), the results obtained by fitting the experimental data are shown in Table 2.

As shown in Table 2, the apparent activation energy and the pre-exponential factor obtained using Coats and Redfern method are 142.9 kJ/mol and 1.6×10^{13} respectively. Zhu et al.²² calculated the apparent activation energy (145.3 kJ/mol) for l-menthol release reaction from its hydroxypropyl- β -cyclodextrin inclusion complex. It indi-

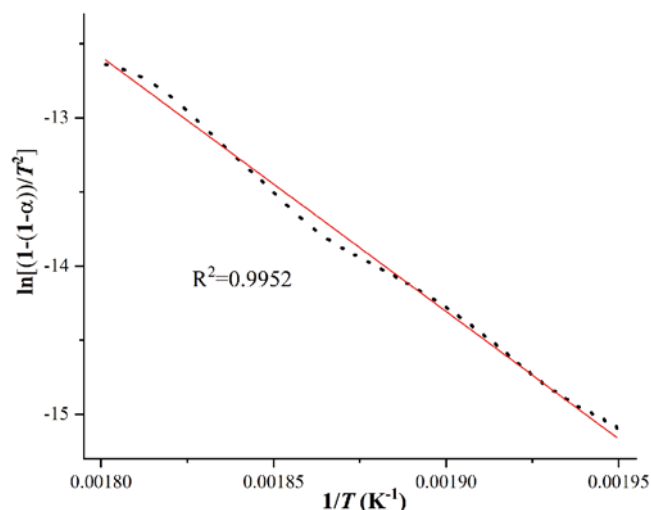


Figure 8. The plot of $\ln[(1-(1-\alpha))/T^2]$ against $1/T$

Table 2. The values of pre-exponential factor and apparent activation energy

Peak T (°C)	T range (°C)	α (%)	E (kJ/mol)	A
267.5	239.8–282.0	0.07–0.99	142.9	1.6×10^{13}

cates that (-)-menthol-hydroxypropyl- β -cyclodextrin inclusion complex is relatively more stable than (-)-menthol- β -cyclodextrin inclusion complex. (-)-Menthol binds relatively more strongly to hydroxypropyl- β -cyclodextrin than to β -cyclodextrin.

Binding energy and structure optimization of menthol- β -cyclodextrin inclusion complex

To some extent, the combination and the interaction between menthol and β -cyclodextrin can be reflected by binding energy, which is defined as the difference between the total energy of menthol- β -cyclodextrin inclusion complex and total energy of menthol and β -cyclodextrin. The total energy includes bend, stretch, stretch-bend, dipole/dipole, torsion, 1,4 van der Waals and non-1,4 van der Waals energy. By successively changing the Z coordinate of menthol, the inclusion process was simulated and the energy was minimized by MM2. When menthol molecule was pushed stepwise through the orifice of β -cyclodextrin, the energy of the complex was minimized at each step. The binding energies calculated by MM2 are shown in Fig. 9.

When the Z coordinate of the C2 in menthol molecule changed from -19.3×10^{-10} m to -12.0×10^{-10} m, only slight changes in binding energy can be observed in Fig. 9. A sharp fall in the value of binding energy occurred when Z coordinate changed from -12.0×10^{-10} m to -9.7×10^{-10} m as shown in Fig. 9. With the increase of Z coordinate of the C2 in menthol molecule, the minimum value of binding energy, -116.7 kJ/mol, was obtained at -0.8×10^{-10} m. The MM2-computed structure of menthol- β -cyclodextrin inclusion complex with the minimum energy is shown in Fig. 10.

When Z coordinate changed from 9.7×10^{-10} m to 10.7×10^{-10} m, a sharp rise in the value of binding energy

Table 1. The squared values of linear correlation coefficient (R^2) for various reaction orders

n	0	0.5	1	1.5	2	2.5	3
R^2	0.9952	0.9822	0.9489	0.8922	0.8264	0.7681	0.7223

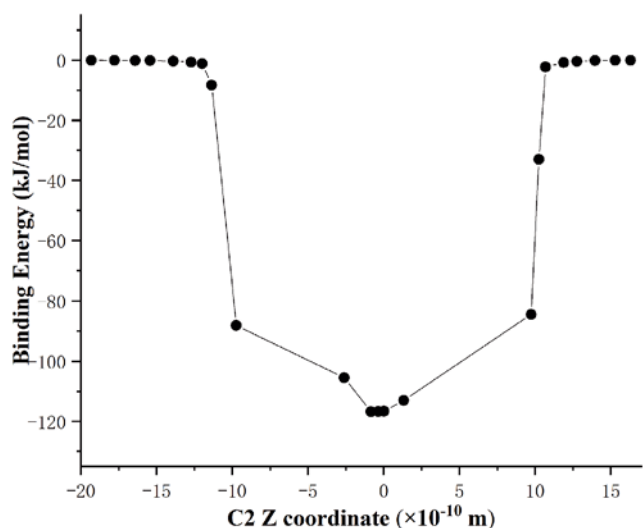


Figure 9. The binding energy calculated by MM2 versus the Z coordinate of the C2 in menthol molecule

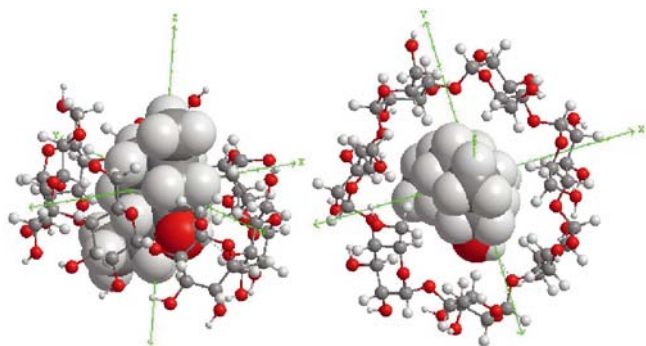


Figure 10. The MM2-computed structure of menthol-β-cyclodextrin inclusion complex with the minimum energy

was observed. As the Z coordinate further increase, the binding energy did not change much. When Z coordinate changed from 10.7×10^{-10} m to 16.3×10^{-10} m, slight changes in binding energy occurred again like the changes from -12.0×10^{-10} m to -19.3×10^{-10} m. The minimum value of binding energy is composed of bend (-2.3 kJ/mol), stretch (-1.7 kJ/mol), stretch-bend (-0.4 kJ/mol), dipole/dipole (-3.1 kJ/mol), torsion (1.4 kJ/mol), 1,4 van der Waals (2.8 kJ/mol) and non-1,4 van der Waals energy change (-113.4 kJ/mol). Non-1,4 van der Waals energy change was the main contribution to binding energy. It is the major reason for the stability of menthol-β-cyclodextrin inclusion complex. However, after the formation of menthol-β-cyclodextrin inclusion complex, the values of torsion and 1,4 van der Waals increase, which are detrimental to the stability of the inclusion complex. Compared the binding energy of menthol-β-cyclodextrin inclusion complex with that of menthol-hydroxypropyl-β-cyclodextrin inclusion complex (-127 kJ/mol)²², the binding energy of menthol-β-cyclodextrin inclusion complex is larger. This indicates that the combination of menthol and β-cyclodextrin is relatively weaker than that of menthol and hydroxypropyl-β-cyclodextrin, and menthol-hydroxypropyl-β-cyclodextrin inclusion complex is relatively more stable than menthol-β-cyclodextrin inclusion complex. This conclusion is consistent with the previous conclusion obtained by pyrolysis activation energy. Compared the binding energy of menthol-β-cyclodextrin inclusion complex with that of difurfuryl disulfide-β-cyclodextrin inclusion complex (-135.2 kJ/

mol)²⁸, the binding energy of difurfuryl disulfide-β-cyclodextrin inclusion complex is the relatively smaller. This indicates that the combination of menthol and β-cyclodextrin is weaker than that of difurfuryl disulfide and β-cyclodextrin. Difurfuryl disulfide-β-cyclodextrin inclusion complex is also relatively more stable than menthol-β-cyclodextrin inclusion complex.

CONCLUSIONS

(-)-Menthol-β-cyclodextrin inclusion complex was successfully fabricated by molecular encapsulation, and was characterized by optical microscopy, FTIR, XRD, and thermogravimetric analysis in this paper. These changes in FTIR and XRD peaks provide evidence that menthol was encapsulated in the cavity of β-cyclodextrin. During the heating process of (-)-menthol itself, it vanished when the temperature exceeded 120 °C. During the pyrolysis of (-)-menthol-β-cyclodextrin inclusion complex, the release of (-)-menthol still occurred before the temperature of initial decomposition of β-cyclodextrin and the maximum (-)-menthol release rate appeared at 267.5 °C. These phenomena confirmed that the formation of inclusion complex can improve the thermo stability of (-)-menthol and provide a long-lasting effect. The reaction order, apparent activation energy and the pre-exponential factor for menthol release reaction were 0 , 142.9 kJ/mol and 1.6×10^{13} respectively. The MM2-computed structure of menthol-β-cyclodextrin inclusion complex with the minimum energy was obtained. The minimum binding energy was -116.7 kJ/mol at -0.8×10^{-10} m. These kinetic parameters and binding energy are helpful to understand the interaction and combination of (-)-menthol and β-cyclodextrin.

ACKNOWLEDGMENTS

This work was financially supported by the National Natural Science Found of China (31972196) and Shanghai Alliance Program (LM201844).

LITERATURE CITED

1. Surburg, H. & Panten, J. (2006). *Common Fragrance and Flavor Materials*. Weinheim, Germany: Wiley-VCH.
2. Burdock, G.A. (2010). *Fenaroli's Handbook of Flavor Ingredients*. Boca Raton, USA: CRC Press. (2010).
3. Hu, Z., Li, S., Wang, S., Zhang, B. & Huang, Q. (2021). Encapsulation of menthol into cyclodextrin metal-organic frameworks: Preparation, structure characterization and evaluation of complexing capacity. *Food. Chem.* 338, 127839. DOI: 10.1016/j.foodchem.2020.127839.
4. Soottitantawata, A., Takayama, K., Okamura, K., Muranaka, D., Yoshiia, H., Furutaa, T., Ohkawarab, M. & Linko, P. (2005) Microencapsulation of l-menthol by spray drying and its release characteristics. *Innov. Food Sci. Emerg.* 6, 163–170. DOI: 10.1016/j.ifset.2004.11.007.
5. Biswas, L., Harrison, E., Gong, Y., Avusula, R., Lee, J., Zhang, M., Rousselle, T., Lage, J. & Liu, X. (2016). Enhancing effect of menthol on nicotine self-administration in rats. *Psychopharmacology* 233, 3417–3427. DOI: 10.1007/s00213-016-4391-x.
6. Lawrence, D., Cadman, B. & Hoffman, A.C. (2011). Sensory properties of menthol and smoking topography. *Tob. Induc. Dis.* 9(Suppl. 1), S3. DOI: 10.1186/1617-9625-9-S1-S3
7. Cadham, C.J., Sanchez-Romero, L.M., Fleischer, N.L., Mistry, R., Hirschtick, J.L., Meza, R. & Levy, D.T. (2020).

The actual and anticipated effects of a menthol cigarette ban: a scoping review. *BMC Public Health* 20, 1055. DOI: 10.1186/s12889-020-09055-z.

8. Wang, H. & Meng, F. (2017). The permeability enhancing mechanism of menthol on skin lipids: a molecular dynamics simulation study. *J. Mol. Model.*, 23, 279. DOI: 10.1007/s00894-017-3457-y.

9. Xu, X., Yu, N., Bai, Z., Xun, Y., Jin, D., Li, Z. & Cui, H. (2011). Effect of menthol on ocular drug delivery. *Graef. Arch. Clin. Exp. Ophthalmol.* 249, 1503–1510. DOI: 10.1007/s00417-011-1703-z.

10. Shen, Q., Li, X., Li, W. & Zhao, X. (2011). Enhanced intestinal absorption of daidzein by borneol/menthol eutectic mixture and microemulsion. *AAPS PharmSciTech* 12(4), 1044–1049. DOI: 10.1208/s12249-011-9672-4.

11. Xia, Q.-p., Chang, L., Mo, Y.-F. & Deng, L. (2020). Experimental study of the influence of menthol on the ozone treatment for corneal alkali burn in rats. *Chinese J. Drug Appl. Monit.* 17(3), 148–151. (in Chinese).

12. Flood, T.R., Waldron, M. & Jeffries, O. (2017). Oral lmenthol reduces thermal sensation, increases workrate and extends time to exhaustion, in the heat at a fixed rating of perceived exertion. *Eur. J. Appl. Physiol.* 117, 1501–1512. DOI: 10.1007/s00421-017-3645-6.

13. Barwood, M.J., Corbett, J., Thomas, K. & Twentyman, P. (2015). Relieving thermal discomfort: Effects of sprayed L-menthol on perception, performance, and time trial cycling in the heat. *Scand. J. Med. Sci. Spor.* 25 (Suppl. 1), 211–218. DOI: 10.1111/sms.12395.

14. Jang, Y.-J., Kim, J.-H. & Lee, J.-Y. (2015). Effects of menthol on thermoregulatory responses after exercise-induced hyperthermia. *Extreme Physiol. Medicine* 4(Suppl 1), A6. DOI: 10.1186/2046-7648-4-S1-A6.

15. Kounalakis, S.N., Botonis, P.G., Koskolou, M.D. & Geladas, N.D. (2010). The effect of menthol application to the skin on sweating rate response during exercise in swimmers and controls. *Eur. J. Appl. Physiol.* 109, 183–189. DOI: 10.1007/s00421-009-1345-6.

16. Wang, Z.-f., Ding, Z.-m., He, J., Ma, Y.-M. & Yang, W.-J. (2020) Progress in chemical constituents, pharmacological activities and product development of mentha haplocalyx Briq. *Mod. Chin. Med.* 22(6), 979–984. DOI: 10.13313/j.issn.1673-4890.20190513002 (in Chinese).

17. Sabzghabae, A.M., Nili, F., Ghannadi, A., Eizadi-Mo-od, N. & Anvari, M. (2011). Role of menthol in treatment of candidial napkin dermatitis. *World J. Pediatr.* 7(2), 167–170. DOI: 10.1007/s12519-011-0253-0.

18. Kong, L., Zuo, H. & Wu, C. (2020). Study on the mechanism of active ingredients of peppermint in the treatment of chronic cholecystitis based on network pharmacology. *Chinese J. Ethnomed. Ethnopharmacology* 29(8), 27–33. DOI:CNKI:SUN:M-ZMJ.0.2020-08-007 (in Chinese).

19. Yoshida, N., Naito, Y., Hirose, R., Ogiso, K., Inada, Y., Fernandopulle, N., Kamada, K., Katada, K., Uchiyama, K., Handa, O., Takagi, T., Konishi, H., Yagi, N., Wakabayashi, N., Yanagisawa, A. & Itoh, Y. (2014). Prevention of colonic spasm using L-menthol in colonoscopic examination. *Int. J. Colorectal Dis.* 29, 579–583. DOI: 10.1007/s00384-014-1844-8.

20. Li, R., Zhang, N., Yao, L. & Li, Y.-h. (2020). Study on the hair growth promotion effect of lavender essential oil and Asian mint essential oil, *China Surfactant Deterg. Cosmet.*, 50(8), 536–541. DOI: 10.3969/j.issn.1001-1803.2020.08.005 (in Chinese).

21. Ferreira, A.I., Silva, W.d.S.e., Neves, L.d.C., Ferreira, N.S., Takata, R. & Luz, R.K. (2020). Benzocaine and menthol as anesthetics for the African cichlid *Aulonocara nyassae*. *Aquacult. Int.*, 28, 1837–1846. DOI: 10.1007/s10499-020-00561-w.

22. Zhu, G., Xiao, Z., Zhu, G., Rujunzhou & Niu, Y. (2016). Encapsulation of l-menthol in hydroxypropyl- β -cyclodextrin and release characteristics of the inclusion complex. *Pol. J. Chem. Technol.* 18, 110–116. DOI: 10.1515/pjct-2016-0056.

23. Yildiz, Z.I., Celebioglu, A., Kilic, M.E., Durgun, E. & Uyar, T. (2018). Menthol/cyclodextrin inclusion complex nanofibers: Enhanced water-solubility and high-temperature stability of menthol. *J. Food Eng.*, 224, 27–36. DOI:10.1016/j.jfoodeng.2017.12.020.

24. Martel, B., Morcellet, M., Ruffin, D., Vinet, F. & Weltrowski, M. (2002). Capture and controlled release of fragrances by CD finished textiles. *J. Incl. Phenom. Macro. Chem.*, 44, 439–442. DOI:10.1023/a:1023028105012.

25. Fernando Ayala-Zavala, J., Soto-Valdez, H., González-León, A., Álvarez-Parrilla, E., Martín-Belloso, O. & González-Aguilar, G.A. (2008). Microencapsulation of cinnamon leaf (*Cinnamomum zeylanicum*) and garlic (*Allium sativum*) oils in β -cyclodextrin. *J. Incl. Phenom. Macrocycl. Chem.*, 60, 359–368. DOI: 10.1007/s10847-007-9385-1.

26. Yoshii, H., Sakane, A., Kawamura, D., Neoh, T.L., Kajiwara, H. & Furuta, T. (2007). Release kinetics of (-)-menthol from chewing gum. *J. Incl. Phenom. Macrocycl. Chem.*, 57, 591–596. DOI: 10.1007/s10847-006-9279-7.

27. Zhu, G., Xiao, Z. & Zhu, G. (2017). Preparation, characterization and the release kinetics of mentha-8-thiol-3-one- β -cyclodextrin inclusion complex. *Polym. Bull.* 74, 2263–2275. DOI: 10.1007/s00289-016-1835-8.

28. Zhu, G., Jiang, X., Zhu, G. & Xiao, Z. (2020). Encapsulation of difurfuryl disulfide in β -cyclodextrin and release characteristics of the guest from its inclusion complex. *J. Incl. Phenom. Macro. Chem.*, 96, 263–273. DOI: 10.1007/s10847-019-00967-x.

29. Zhu, G., Feng, N., Xiao, Z., Zhou, R. & Niu, Y. (2015). Production and pyrolysis characteristics of citral-monochlorotriazinyl- β -cyclodextrin inclusion complex. *J. Therm. Anal. Calorime.*, 120, 1811–1817. DOI:10.1007/s10973-015-4498-z.

30. Saenger, W., Jacob, J., Gessler, K., Steiner, T., Hoffmann, D., Sanbe, H., Koizumi, K., Smith, S.M. & Takaha, T. (1998). Structures of the common cyclodextrins and their larger analogues beyond the doughnut. *Chem. Rev.* 98, 1787–1802. DOI: 10.1021/cr9700181.

31. Polarz, S., Smarsly, B., Bronstein, L. & Antonietti, M. (2001) From Cyclodextrin Assemblies to Porous. *Angew. Chem. Int. Ed.* 40, 4417–4421. DOI: 10.1002/1521-3773(20011203)40:23<4417::AID-ANIE4417>3.0.CO;2-P.

32. Zhu, G., Zhu, G. & Xiao, Z. (2019). A review of the production of slow-release favor by formation inclusion complex with cyclodextrins and their derivatives. *J. Incl. Phenom. Macro. Chem.* 95, 17–33. DOI: 10.1007/s10847-019-00929-3.